Vol 16 No 8, August 2007
1009-1963/2007/16(08)/2343-06

Chinese Physics

© 2007 Chin. Phys. Soc.
and IOP Publishing Ltd

International Linear Collider damping ring lattice design with two wiggler sections*

Sun Yi-Peng(孙一鹏)[a)b)†], Gao Jie(高 杰)[b)], and Guo Zhi-Yu(郭之虞)[a)]

[a)] *Key Laboratory of Heavy Ion Physics (MOE) and School of Physics, Peking University, Beijing* 100871, *China*

[b)] *Institute of High Energy Physics, Chinese Academy of Science, Beijing* 100049, *China*

(Received 10 October 2006; revised manuscript received 27 December 2006)

The International Linear Collider (ILC), which is based on super-conducting RF acceleration technology, requires the damping rings to provide beams with extremely small equilibrium emittance, and large acceptance to ensure good injection efficiency for high-emittance, and high-energy spread beam from the positron source. In order to reduce the cost for ILC damping rings, an alternative lattice which is different from the baseline configuration design has been designed with modified FODO arc cells, and the total quadrupole number has been reduced by half. At the same time, to decrease the total cost involved in constructing access shafts needed to supply power, cryogenics etc. for the wigglers and other systems, the number of wiggler sections is decreased from 8 to 4, and further to 2. This new lattice has been optimized to have a good dynamic aperture. This alternative ILC damping ring lattice design will reduce the cost largely as compared with the baseline design.

Keywords: ILC damping ring, FODO arc cell, wiggler sections, dynamic aperture
PACC: 2900, 2920, 2921

1. Introduction

The International Linear Collider (ILC) damping rings should provide beams with very low natural emittance for the linear collider to reach the required luminosity, and at the same time, the damping rings also need to have a large acceptance to ensure good injection efficiency for high-emittance, high-energy spread beam from the positron source.[1] Another main design criterion for the damping ring comes from the requirement of providing a long beam pulse of 1 ms containing 2820 bunches (normal parameter set[2]), corresponding to an approximately 300 km long bunch train. To keep the damping ring's circumference reasonable, the bunch train has to be stored in a compressed mode with a much smaller bunch spacing than in the linacs. Consequently, each bunch has to be individually injected and ejected. The ring circumference is then determined both by the pulse width of the injection and extraction kicker system and the electron-cloud (ion) effects. Based on the studies of the various configuration options, the ILC damping ring baseline configuration design (BCD) decides that the positron damping ring should consist of two (roughly circular) rings of approximately 6 km circumference in a single tunnel and the electron damping ring should consist of a single 6 km ring, assuming that the fill pattern allows a sufficient gap for clearing ions.[2,3]

In the ILC damping ring baseline design, a lattice which has a circumference of approximately 6 km using theoretical minimum emittance arc cells has been used.[4] In this paper, with the aim to reduce the cost of the damping rings, a new lattice with modified FODO arc cells is designed as an alternative of the baseline design. To decrease the total cost involved in constructing access shafts needed to supply power, cryogenics etc. for the wigglers and other systems, the number of wiggler sections is decreased from 8 to 4, and further to 2.

In the following sections, the linear lattice design, the chromaticity correction, and the dynamic aperture optimization of the damping ring lattice with two wiggler sections will be presented.

2. The linear lattice design of the damping ring

*Project supported by the National Natural Science Foundation of China (Grant No 10525525).
†E-mail: ypsun@ihep.ac.cn

2.1. The lattice of the arc cell and the dispersion suppressor

There are 120 arc cells in all for a 6 km damping ring, therefore each arc cell provides a bending angle of $\pi/60$ for the beam. The FODO arc cell length is selected to be 38.9 m and the phase advance per arc cell is 90°/90° for the horizontal and vertical betatron motions, respectively. According to Eq.(1), the maximum and the minimum values of the beta functions of the FODO arc cell is 66.2 m and 11.4 m, respectively. From Eq.(2), the maximum and the minimum horizontal dispersion functions are 1.37 m and 1.02 m respectively, which are too large to obtain a reasonable bunch length of 6 mm.

$$\beta^{\pm} = \frac{L_{\rm P}\left(1 \pm \sin\frac{\mu}{2}\right)}{\sin\mu}, \tag{1}$$

$$D^{\pm} = \frac{L_{\rm P}\phi\left(1 \pm \frac{1}{2}\sin\frac{\mu}{2}\right)}{4\sin^2\frac{\mu}{2}}, \tag{2}$$

where β^+ and β^- are the maximum and minimum values of the beta functions, D^+ and D^- are the maximum and minimum values of the horizontal dispersion functions, $L_{\rm P}$ is the length of the cell, μ is the phase advance of the cell, and ϕ is the bending angle in one arc cell. To have smaller RMS dispersion value, the length of the drifts between the quadrupoles is adjusted and the ultimate values of the two long drifts are 13.7 m and 1.55 m with the maximum and the RMS horizontal dispersion functions being 1.15 m and 0.77 m, respectively.

The lattice functions in an arc cell are shown in Fig.1.

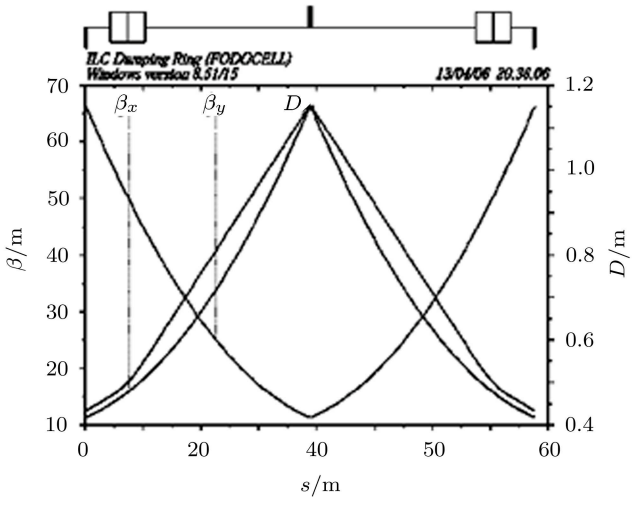


Fig.1. Lattice functions in an arc cell.

The dispersion suppressors match the dispersion function between arc sections and straight sections. There are two kinds of dispersion suppressor insertions. One matches the dispersion function without affecting the alpha and beta functions, and the other suppresses the dispersion function by only modifying the focal length of two quadrupoles, which modifies both the alpha and beta functions. Here we do not use the usual method to make a dispersion suppressor, but insert three quadrupoles into the arc cell to obtain a dispersion suppressor, as shown in Fig.2.

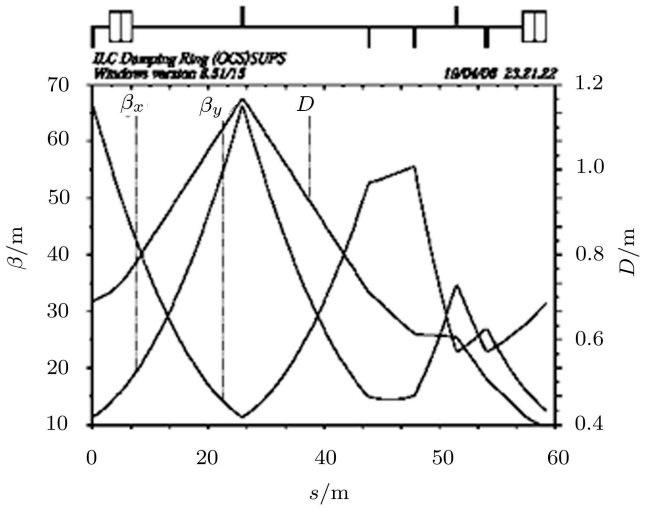


Fig.2. Lattice functions in a dispersion suppressor.

2.2. The lattice of the RF and wiggler cell

The vertical damping time can be written as follows:

$$\tau_y = \frac{3C}{r_{\rm e}c\gamma^3 I_2} = \frac{3C}{r_{\rm e}c\gamma^3(I_{\rm 2d} + I_{\rm 2w})}, \tag{3}$$

where C is the circumference, $r_{\rm e}$ is the classical radius of an electron, c is the speed of light, γ is the relativistic factor, and I_2 is the second synchrotron integral over dipoles and wigglers.

The equilibrium horizontal emittance can be written as

$$\gamma\varepsilon_x = \frac{C_q\gamma^3 I_5}{J_x I_2}, \tag{4}$$

where $C_{\rm q} \approx 3.84\times10^{-13}$ m, $J_x \approx 1$ for a separate function magnet, and I_5 is determined by the arc sections. The wiggler section is designed to provide enough damping. The average beta functions in this section are about 10 m, and a total of 40 such wiggler sections have been used for positron damping ring. The lattice

functions in a RF cell and in a wiggler cell are shown in Fig.3.

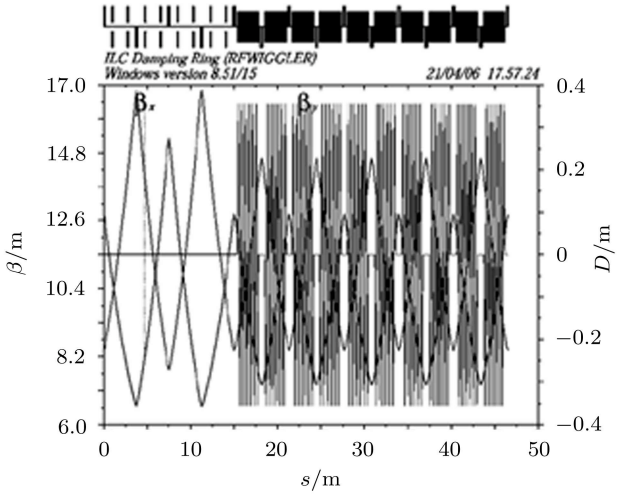


Fig.3. Lattice functions in the RF and wiggler cells.

2.3. The lattice of the straight sections

There are two long straight sections which are designed to be dispersion free. One is designed for the injection and the extraction of the beam. The incoming electrons (or positrons) are injected into the empty RF buckets in the ring, rather than being added to the contents of bunches already orbiting the ring. In addition, the emittance of an incoming positron bunch is very large. As a result, the injection and extraction optics must be designed to accommodate these beam characteristics while still achieving high injection and extraction efficiencies.

The injection and extraction optics are designed to accommodate either of the two different types of kickers that are studied at Fermilab: a pulsed kicker system with 6 ns rise time (and a longer fall time) and a Fourier kicker, which is shown in Fig.4.[5]

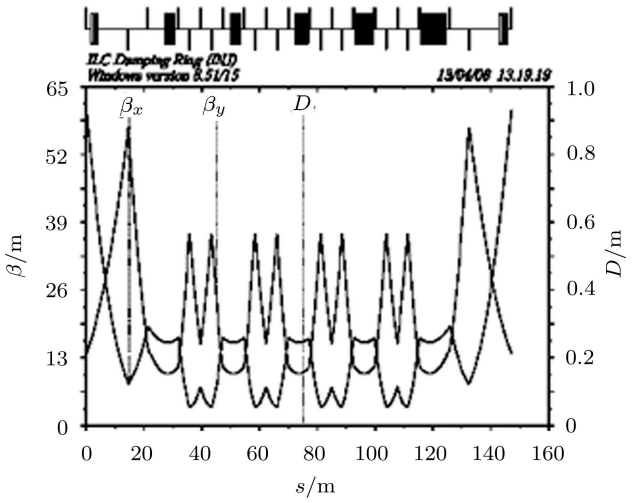


Fig.4. The injection and extraction lattices.

2.4. The whole ring

There are totally four long straight sections in the ring. The RF cavities and the wigglers have been installed in two of them. The layout of the ring has been designed with 4-fold symmetry. The lattice functions for the whole ring and the layout of the lattice are shown in Fig.5 and the principal lattice parameters are listed in Table 1.

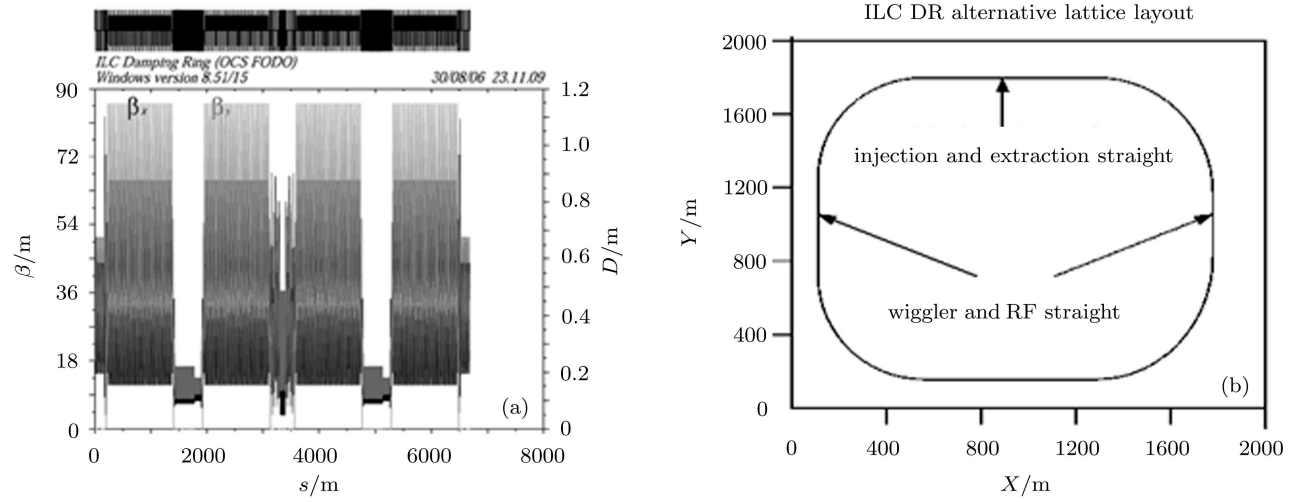


Fig.5. (a) Lattice functions for the whole ring; (b) Layout of the lattice.

Table 1. The principal lattice parameters.

Circumference/m	6695.057
Harmonic number	14516
Energy/GeV	5
Arc cell	FODO
Tune	48.35/45.32
Natural chromaticity	$-59/-61$
Momentum compaction/10^{-4}	4
Transverse damping time/ms	25/25
Norm. Natural emittance/mm-mrad	4.2
RF voltage/MV	46.6
Synchrotron tune	0.093
Synchrotron phase/(°)	169.2
RF frequency/MHz	650
RF acceptance/%	2.68
Natural bunch length/mm	5.96
Natural energy spread/10^{-3}	1.28

3. Chromaticity correction and frequency map analysis

3.1. Chromaticity correction and dynamic aperture

Two family sextupoles in the arc cell are used to correct the first-order chromaticity to above zero. The phase advance per arc cell is 90°/90° for the horizontal and vertical betatron motions, respectively. There are totally four arc sections and thirty arc cells in each arc section. Therefore, the phase advance per arc section is 15π for both the horizontal and vertical betatron motions. This kind of second-order achromat helps to cancel all driving terms of the third-order resonances generated by the sextupoles within each arc section.

However, as the number of wiggler sections is decreased from 8 to 2, the symmetry of the whole lattice is decreased from 10- to 4-fold. That will make the optimization of the dynamic aperture harder. So the phase advance of each straight section and the total tune of the ring should be carefully selected. The phase advance between the arc sections, that is to say in straight sections, also plays a dominant role in determining the dynamic aperture. Roughly, it is thought that the best phase advance in the straight section is nearly a multiple of 360°, which makes the whole straight section an identity transformation and therefore maximizes the symmetry of the ring and minimizes the number of excited high order resonances.[6]

In our study it is found that not only the phase advance in the straight section but also the phase advance between the last sextupole in one arc section and the first sextupole in the next arc section are very important. The straight sections are optimized to give a reasonable horizontal phase advance which is near 2π, and a vertical phase advance which is near π.

The position of the two family of sextupoles in the arc cell has been adjusted to give a good chromaticity property and a larger dynamic aperture. The variation of tune with momentum spread ±1% is shown in Fig.6(a). After tracking for 1024 turns, the dynamic apertures of both on-momentum and off-momentum particles are obtained, as shown in Fig.6(b).[7]

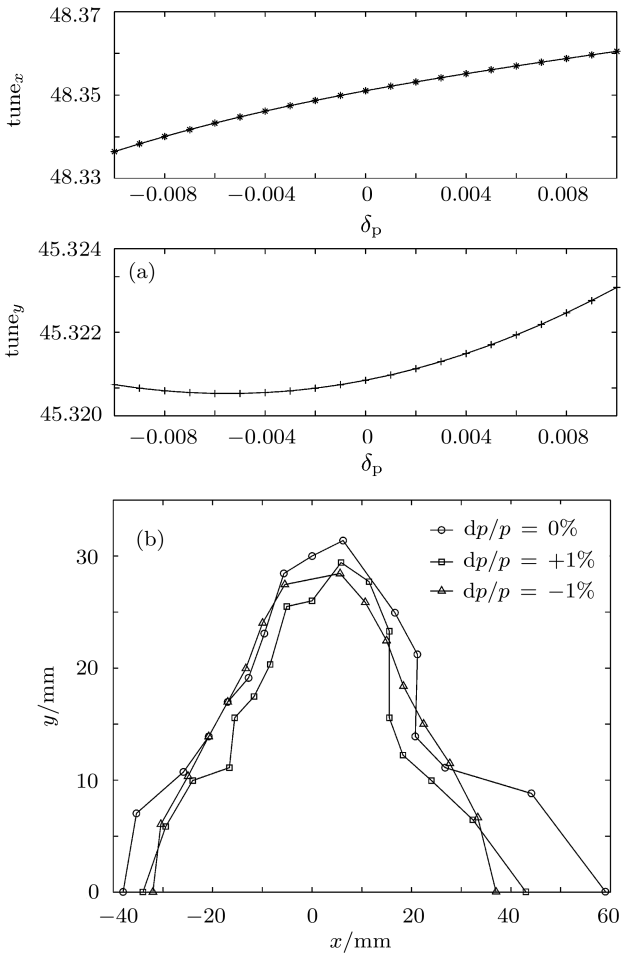


Fig.6. The tune variation with momentum spread ±1% (a); the dynamic aperture with momentum spread up to ±1% (b).

It can be calculated from the injected beam's emittance and the beta functions at the injection point of the ring, that the horizontal and vertical bunch sizes of the injected beam are approximately 6.6 and 4.2 mm, respectively. It can be seen from Fig.6(b) that the dynamic aperture is nine times the verti-

cal injected beam size and seven times the horizontal injected beam size for on-momentum particles. The lattice also gives a good dynamic aperture for off-momentum particles.

As the nonlinear wiggler effect is not included in the tracking process, we use an analytical method to calculate the dynamic aperture of the damping ring with ideal nonlinear wigglers.[8] One has the dynamic aperture limited by one wiggler as follows (vertical and horizontal respectively):

$$A_{N_{\rm w},y}(s) = \sqrt{\frac{3\beta_y(s)}{\beta_{y,m}^2}}\frac{\rho_{\rm w}}{k_y\sqrt{L_{\rm w}}}, \tag{5}$$

$$A_{N_{\rm w},x}(s) = \sqrt{\frac{\beta_y(s)}{\beta_x(s)}(A_{N_{\rm w},y}^2(s) - y^2)}\ , \tag{6}$$

where $\beta_y(s)$ and $\beta_x(s)$ are the unperturbed beta functions at the tracking point, $\beta_{y,m}$ is the vertical beta function at the middle of the wiggler, $\rho_{\rm w}$ is the radius of curvature of the wiggler peak magnetic field B_0, $L_{\rm w} = N_{\rm w}\lambda_{\rm w}$ is the wiggler length, $k_y = 2\pi/\lambda_{\rm w}$, $\lambda_{\rm w}$ is the period length of the wiggler, and $N_{\rm w}$ is the cell number of a wiggler.

Assuming that the dynamic aperture of the ring without the wiggler's effects is A_y and that there are M wigglers to be inserted inside the ring at different places, one has the total dynamic aperture expressed as

$$A_{{\rm total},y}(s) = \frac{1}{\sqrt{\dfrac{1}{A_y^2(s)} + \displaystyle\sum_{j=1}^{M}\frac{1}{A_{j,{\rm w},y}^2(s)}}}\ , \tag{7}$$

where $A_{j,{\rm w},y}$ denotes the dynamic aperture limited by the j-th wiggler.

Using Eqs.(5), (6) and (7), the dynamic apertures including nonlinear wiggler effects of both on-momentum and off-momentum particles are shown in Table 4, where off-momentum particles' dynamic aperture is also calculated. A_{y0} and A_{x0} are the vertical and horizontal dynamic apertures in linear wiggler model. A_y and A_x are the corresponding vertical and horizontal dynamic apertures including nonlinear wiggler effects.

Table 2. Dynamic aperture using nonlinear wiggler.

dp/p	A_y/mm	A_x/mm	A_{y_0}/mm	A_{x_0}/mm
0	21	47	32	60
−1%	20.2	34	30	43

It can be seen from Table. 2 that the dynamic aperture of the designed damping ring, where nonlinear wiggler effect has been taken into account, is greater than five times the injected beam size for on-momentum particles and five times the injected beam size for off-momentum particles. These results can fulfill the requirement of three times the injected bunch size.

3.2. Frequency map analysis results

Frequency map analysis (FMA) is introduced for the demonstration and understanding of the chaotic behaviour of a dynamical system. The application to particle accelerator dynamics is done in the case that the motion of a single particle in a storage ring is described in a surface of section of the beam by a symplectic map of dimension 4 or 6.[9] Here FMA is used to optimize the working points and the dynamic aperture. The optimized result is shown in Fig.7, where 2500 particles distributed in the range of seven times the injected bunch size are tracked for 1024 turns to do FMA on the lattice.

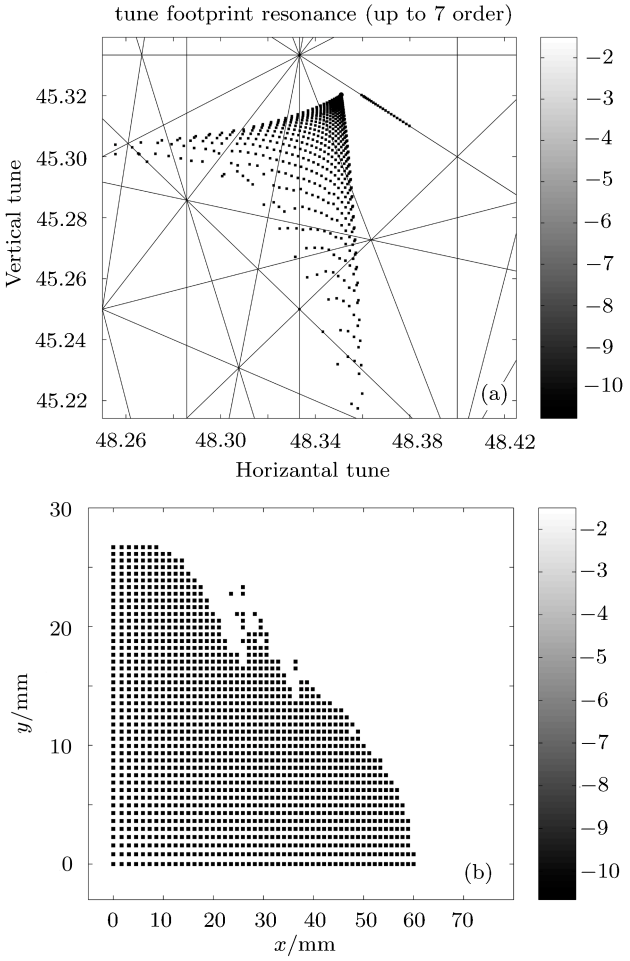


Fig.7. FMA for damping ring dynamic aperture: (a) footprint; (b) dynamic aperture with FMA.

4. Conclusion

An alternative damping ring lattice with modified FODO arc cells and only two wiggler sections has been designed to reduce the cost of ILC damping rings. The number of quadrupoles in the whole ring has been decreased by half compared with the original ILC damping ring BCD design. Also the number of access shafts needed to supply power, cryogenics etc. for the wigglers and other systems, is decreased from 8 to 2. The circumference, the equilibrium emittance, the bunch length, the acceptance, the dynamic aperture, and the damping time can fulfill the requirements for the ILC damping ring. The dynamic aperture is large enough with the nonlinear wiggler effects taken into account. Frequency map analysis has been used on this lattice during the optimization of the dynamic apertures by choosing the working point far away from the dangerous resonance lines. Next, the phase advance of the arc cell will be varied to study the lattice with a lower momentum compaction, 2×10^{-4}, which is connected with the requirements of the instability estimation.

Acknowledgments

The author would like to thank Xu G., Qin Q, Jiao Y for their helpful discussions.

References

[1] Gao J 2006 *High Energy Physics and Nuclear Physics* **30** Supp 156
[2] Wolski A, Gao J and Guiducci S 2006 *EPAC* 06
[3] ILC BCD 2006 http://www.linearcollider.org/
[4] Xiao A 2004 Fermilab Technical Report
[5] Emery L and Kim K J 2004 *FERMILAB-TM-2272-AD-TD*
[6] Cai Y 2004 SLAC-PUB-11084
[7] Terebilo A 2001 SLAC-PUB 8732
[8] Gao J 2000 *Nucl. Instrum. Methods* A **451** 545
[9] Dumas S and Laskar J 1993 *Phys. Rev. Lett.* **70** 2975